Available online at www.sciencedirect.com

ScienceDirect

Mendeleev Commun., 2022, **32**, 488–491

Mendeleev Communications

Selective hydrogenation of α,β-unsaturated aldehydes over Pt supported on cerium–zirconium mixed oxide of different composition

Kseniia V. Vikanova,*[a] Elena A. Redina,[a] Gennady I. Kapustin,[a] Igor V. Mishin,[a] Nikolay A. Davshan[a] and Leonid M. Kustov[a,b,c]

[a] *N. D. Zelinsky Institute of Organic Chemistry, Russian Academy of Sciences, 119991 Moscow, Russian Federation. E-mail: ks.vikanova@gmail.com*
[b] *National University of Science and Technology 'MISiS', 119049 Moscow, Russian Federation*
[c] *Department of Chemistry, M. V. Lomonosov Moscow State University, 119991 Moscow, Russian Federation*

DOI: 10.1016/j.mencom.2022.07.019

Cerium–zirconium mixed oxides with different Ce/Zr ratio were prepared and used as supports for Pt-containing catalysts. The study of the catalysts in the cinnamaldehyde hydrogenation reaction has shown that cinnamaldehyde conversion and cinnamyl alcohol selectivity strongly depend on the CeO_2 content in the support. The highest cinnamyl alcohol yield of 81% was obtained in 105 min at room temperature and atmospheric pressure over the 1%Pt/CeO_2–ZrO_2 catalyst with Ce : Zr atomic ratio equal to 4 : 1.

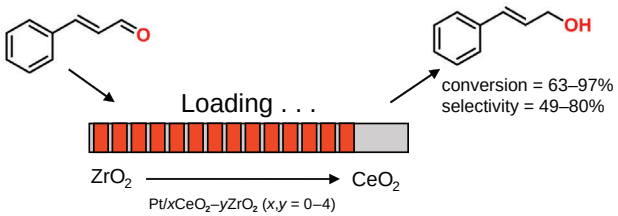

Keywords: cinnamaldehyde, cinnamyl alcohol, cerium oxide, zirconium oxide, selective hydrogenation, unsaturated alcohol synthesis, platinum, α,β-unsaturated aldehydes.

Selective hydrogenation of α,β-unsaturated aldehydes is of great interest both for the chemical industry and organic synthesis as it allows one to obtain alcohols of various structures according to the substrate used.[1–3] The main problem of the hydrogenation of such substrates is the presence of conjugated C=O carbonyl group and C=C bond, with the reactivity of the latter being higher than that of the carbonyl bond.[4,5] Therefore, the development of an active and selective catalytic system is a major challenge to the researchers.

The nature of the support and its composition largely determine both the activity and selectivity of the catalyst.[6] Cerium(IV) oxide is widely used as a catalyst support because of its unique capability to oxidation and reduction with the formation of Ce_2O_3 and strong metal–support interaction (SMSI).[7] The addition of zirconium oxide intensifies the CeO_2 redox cycle and enhances the SMSI effect.[8,9] The high activity and selectivity of Pt/CeO_2–ZrO_2 catalysts in the number of hydrogenation processes has been shown by our group earlier.[10,11] Nevertheless, the data on the optimal Ce/Zr ratio are contradictory, since this value depends on the synthesized catalyst and the process it is used for.[12,13] In this work, catalysts with the composition 1%Pt/$x$$CeO_2$–$y$$ZrO_2$ were studied in cinnamaldehyde selective hydrogenation as model reaction of α,β-unsaturated aldehydes hydrogenation at room temperature and atmospheric pressure.[†]

According to the SEM study, the CeO_2–ZrO_2 samples resemble a loose structure (see Figure 1). EDX mapping has revealed a uniform distribution of CeO_2 and ZrO_2 over the surface of all carriers, regardless of the component ratio.

X-ray diffraction patterns of individual zirconium oxide indicate the presence of two phases: ZrO_2 monoclinic (2θ = 24.0°, 28.2° and 31.3°) and ZrO_2 tetragonal (2θ = 30.2° and 35.1°)[14] (see Figure 2). The addition of a small amount of CeO_2 results in a slight shift in the position of the reflections of tetragonal ZrO_2 to the region of smaller angles and simultaneous

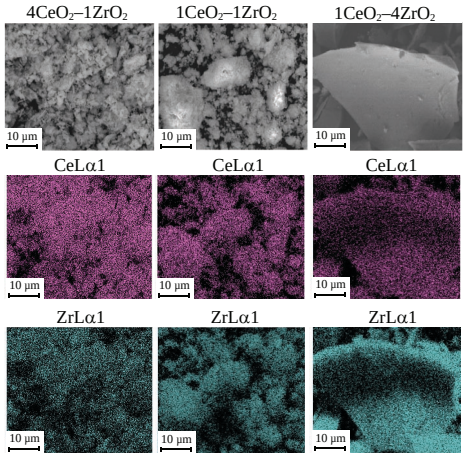

Figure 1 SEM + EDX images of elements distribution in mixed $x$$CeO_2$–$y$$ZrO_2$ supports.

[†] The synthesis of $x$$CeO_2$–$y$$ZrO_2$ supports (where x, y – atomic ratio Ce : Zr; x, y = 0–4) was carried out by coprecipitation of metal precursors. Catalysts with 1 wt% of Pt were synthesized by pH-controlled precipitation. The prepared materials were characterized by SEM-EDX, XRD, BET and temperature programmed reduction (TPR-H_2) methods. The liquid-phase cinnamaldehyde hydrogenation reaction was carried out at atmospheric pressure and room temperature (25 °C). The preparation and characterization techniques, as well as typical reaction and analysis products procedures, are given in details in Online Supplementary Materials.

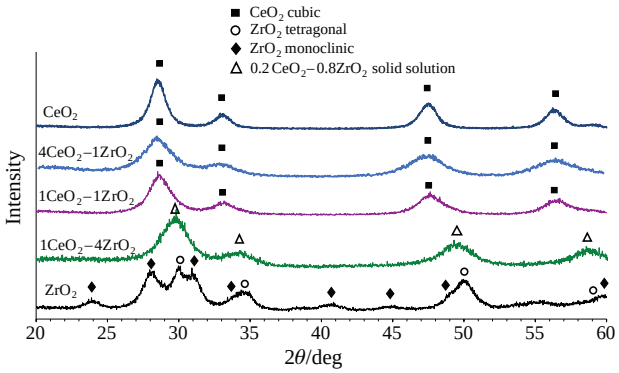

Figure 2 X-ray diffraction patterns of $x CeO_2$–$y ZrO_2$ carriers.

increase of the ZrO_2 lattice parameter, which indicates the formation of a solid solution based on the tetragonal zirconium oxide phase.[15,16] In this case no traces of the ZrO_2 monoclinic phase were found. This effect was described earlier; it was noted that addition of a small amount of diverse oxides, including CeO_2, stabilizes the ZrO_2 tetragonal phase.[17–19]

The increase in the amount of the cerium component in mixed oxides leads to phase segregation and crystallization of CeO_2 particles. Peaks at 2θ = 28.5°, 33.1°, 47.5° and 56.3° are clearly observed in $1CeO_2$–$1ZrO_2$ and $4CeO_2$–$1ZrO_2$ samples, thus indicating the presence of a CeO_2 cubic phase, whereas ZrO_2 is amorphous. The calculated lattice parameter for these supports coincides with the lattice parameter of the individual cerium oxide (see Table 1). Therefore, XRD results showed that at the cerium oxide concentrations exceeding 20% the phase segregation occurs with the formation of CeO_2 and ZrO_2 individual phases.

The TPR-H_2 studies of the prereduced catalysts have shown that hydrogen uptake by the 1%Pt/ZrO_2 catalyst was close to the stoichiometric value (see Table 2). For the samples supported on Ce-containing carriers the consumption of hydrogen started at the temperature of –50 °C. The values of H_2 uptake per mol of Pt were several times higher than the stoichiometric ones. This phenomenon can be explained by spillover of hydrogen dissociated at the primary centers of Pt onto the support.[20] It causes the partial reduction of Ce^{4+} ions to Ce^{3+} and the formation of an oxygen vacancy in the metal–support interface region, which may act as selective C=O bond adsorption centrum. An intensification of H_2 uptake was observed at the increase of cerium content in the support reaching a maximum for the 1%Pt/$4CeO_2$–$1ZrO_2$ catalyst. A similar effect on unreduced Pt-containing catalysts was described by Damyanova *et al.*[21] Authors noted an increase of the H_2 adsorption peak during Pt

Table 1 Morphological parameters of prepared supports.

Support	S_{BET}/ m^2 g^{-1}	Support phase composition (XRD)	Crystallite size (XRD)/Å	Lattice parameter/Å
ZrO_2	98	ZrO_2 tetragonal ZrO_2 monoclinic	60 55	3.598 5.312
$1CeO_2$–$4ZrO_2$	98	$Ce_{0.2}Zr_{0.8}O_2$ tetragonal	50	3.640
$1CeO_2$–$1ZrO_2$	90	CeO_2 cubic ZrO_2 amorphous	55	5.410
$4CeO_2$–$1ZrO_2$	103	CeO_2 cubic ZrO_2 amorphous	50	5.410
CeO_2	103	CeO_2 cubic	60	5.410

Table 2 TPR-H_2 data on prereduced Pt-contained catalysts in the temperature range from –50 to +25 °C.

Catalyst	H_2 uptake/ mmol g^{-1}	H_2/Pt ratio (mol/mol)
1%Pt/ZrO_2	0.03	1.15
1%Pt/$1CeO_2$–$4ZrO_2$	0.46	8.99
1%Pt/$1CeO_2$–$1ZrO_2$	0.47	9.18
1%Pt/$4CeO_2$–$1ZrO_2$	0.67	13.06
1%Pt/CeO_2	0.65	12.78

reduction in the temperature range 150–200 °C with an increase of Ce content in the support. Hence, it is safe to assume that the higher cerium oxide content leads to an increase of Pt–CeO_2 interface areas and to the formation of larger amounts of Ce^{3+} sites.

However, the H_2 uptake by the catalyst based on CeO_2 turned out to be lower than that for the $4CeO_2$–$1ZrO_2$ mixed oxide, which indicates the intensification of hydrogen spillover upon the addition of zirconium oxide to CeO_2. A number of researchers noted that addition of Zr to CeO_2 facilitates the transport of oxygen from the bulk to the surface, affecting the amount of hydrogen required for reduction.[22–24] Thus, the increase of the CeO_2 content results in the increase of hydrogen uptake, whereas addition of small ZrO_2 amount intensifies reduction of cerium oxide.

The catalysts were examined in the selective hydrogenation of cinnamaldehyde (CAld) **1** at room temperature and atmospheric pressure. Possible reaction products: hydrocinnamaldehyde (HCAld) **2**, cinnamyl alcohol (CAlc) **3** and hydrocinnamyl alcohol (HCAlc) **4** are shown in Scheme 1.

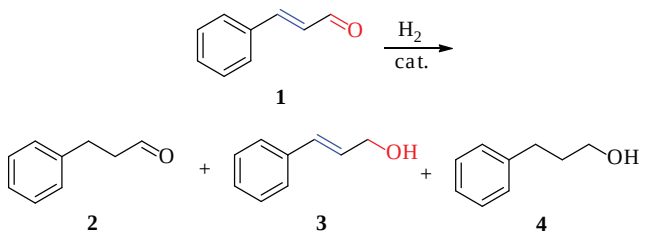

Scheme 1

Dependence of the catalysts activity and selectivity *vs.* Ce/Zr ratio is illustrated in Figure 3. The increase of ceria content from 20 to 80% results in the rise of cinnamaldehyde **1** conversion from 67 to 97% with the growth of cinnamyl alcohol **3** selectivity from 63 to 80%. Wei *et al.*[7] also reported the higher product **3** yield with the rise of the Ce content in the carrier, which reaches a maximum of 90% on the Pt/50%CeO_2–50%ZrO_2 catalyst at the H_2 pressure of 1.0 MPa and temperature of 60 °C. The authors explained this dependence by growth of the number of oxygen vacancies in the supports with enlarging amount of cerium oxide. However, it was found that at further increase of the CeO_2 content both conversion of compound **1** and selectivity of product **3** decreased. We observed the growth of the conversion and selectivity with the increase of the CeO_2 content and the drop of activity when using the catalyst supported on individual CeO_2. Thereby, we can also assume that an increase in the CeO_2 content in the sample leads to a growth of the oxygen vacancies number during Ce^{4+} to Ce^{3+} reduction, but at the same time the addition of ZrO_2 also strongly affects on the activity of the catalyst. Earlier, for 5-(hydroximethyl)furfural hydrogenation reaction in the presence of Pt-containing systems based on Ce–Zr supports we noted that addition of a small amount of ZrO_2 also leads to a rise of activity and selectivity of the samples. This effect might be

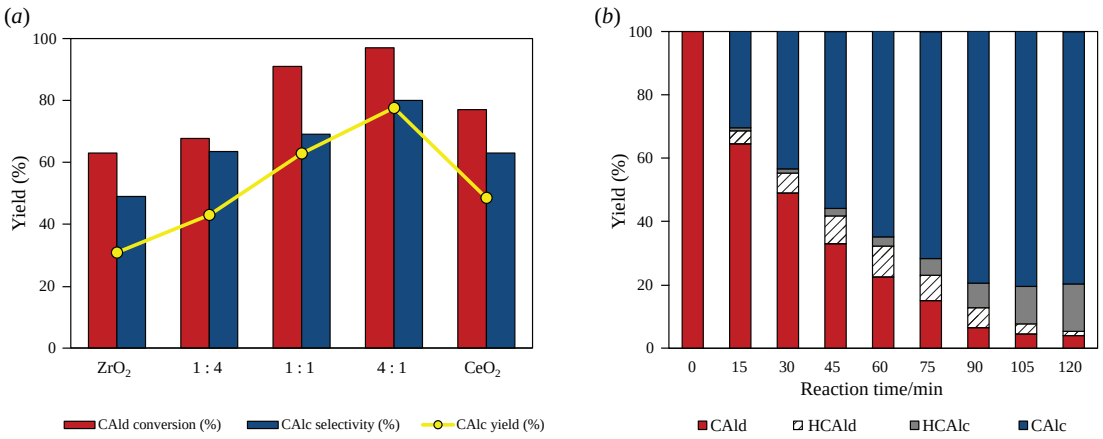

Figure 3 (*a*) CAld conversion and CAlc selectivity on Pt catalysts based on different xCeO$_2$–yZrO$_2$ supports and (*b*) reaction products distribution on the 1%Pt/4CeO$_2$–1ZrO$_2$ catalyst.

caused by the electron deficient sites formation on the CeO$_2$/ZrO$_2$ phases boundary, which, probably, also take part in the substrate adsorption. The highest substrate conversion and cinnamyl alcohol **3** selectivity were obtained on the 1%Pt/4CeO$_2$–1ZrO$_2$ catalyst.

The product distribution *vs.* time in the presence of 1%Pt/4CeO$_2$–1ZrO$_2$ has shown that the highest cinnamyl alcohol **3** yield (81%) was achieved after 105 min of the reaction. However, a further increase in the reaction time led to the drop of the unsaturated alcohol selectivity and to the increase in the amount of the C=C bond hydrogenation product. To estimate the specific activity of the samples, turnover frequency (TOF) values were calculated considering 15 min of the reaction (Table 3). The highest TOF value (166 h^{-1}) was obtained for the 1%Pt/4Ce$_2$–1ZrO$_2$ sample. Zhang *et al.*[25] reported that maximum TOF value of 77 h^{-1} was achieved in cinnamaldehyde **1** hydrogenation at 40 °C and hydrogen pressure of 3 MPa with the use of Pt–Ni nanowires encapsulated by MOF. Machado *et al.*[26] obtained TOF value of 86 h^{-1} in the presence of 1% Pt catalyst based on Li-doped carbon aerogel at reaction temperature 90 °C and H$_2$ pressure of 1.0 MPa.

To evaluate the prospects of industrial use of these catalytic systems, we calculated the molar productivity values (see Table 3). The sample of 1%Pt/4CeO$_2$–1ZrO$_2$ catalyst has shown the greatest molar productivity (135 h^{-1}) . Yoon *et al.* achieved the molar productivity value of 107 h^{-1} on Ru-based porous organic polymer in cinnamaldehyde hydrogenation at 30 °C and P_{H2} = 1 MPa.[27]

In conclusion, Pt-containing catalysts based on CeO$_2$–ZrO$_2$ supports with different Ce/Zr ratios were examined in the cinnamaldehyde hydrogenation reaction. The highest cinnamaldehyde conversion (97%) and cinnamyl alcohol selectivity (80%) were obtained on the catalyst supported over the 4CeO$_2$–1ZrO$_2$ carrier. Direct correlation between the catalyst activity/selectivity and CeO$_2$ content in the mixed supports was found. The TPR-H$_2$ data showed that the 1%Pt/4CeO$_2$–1ZrO$_2$ catalyst exhibited the highest H$_2$ consumption among all catalysts used. Thus, an increase of the cerium content in the support leads to the growth of H$_2$ uptake and, probably, to an increase of the amount of Ce^{3+} sites, which may act as the centers of C=O bond selective adsorption. The addition of zirconia not only intensifies the reduction of CeO$_2$, but also, presumably, contributes to the formation of additional active centers at the Pt–CeO$_2$–ZrO$_2$ interface.

Table 3 Turnover frequency and molar productivity values of 1%Pt/xCeO$_2$–yZrO$_2$ catalysts.

Catalyst	TOF[a]/h^{-1}	Molar productivity[b]/h^{-1}
1%Pt/ZrO$_2$	51	36
1%Pt/1CeO$_2$–4ZrO$_2$	69	54
1%Pt/1CeO$_2$–1ZrO$_2$	158	122
1%Pt/4CeO$_2$–1ZrO$_2$	166	135
1%Pt/CeO$_2$	120	68

[a] TOF calculated as cinnamaldehyde **1** (mmol) transformed during the reaction per 1 mmol of Pt per hour. [b] Molar productivity calculated as cinnamyl alcohol **3** (mmol) formed during the reaction per 1 mmol of Pt per hour.

The work was supported by Russian Science Foundation (grant no. 17-73-20282) in the part related to catalytic studies and Ministry of Science and Higher Education of Russian Federation (grant no. 075-15-2021-591) in the part related to catalyst preparation and characterization. Scanning electron microscopy was performed in the Department of Structural Studies of N. D. Zelinsky Institute of Organic Chemistry, Moscow.

Online Supplementary Materials

Supplementary data associated with this article can be found in the online version at doi: 10.1016/j.mencom.2022.07.019.

References

1 P. Liu, Y.-L. Zhu, L. Zhou, W.-H. Zhang and Y.-X. Li, *Catal. Lett.*, 2020, **150**, 2695.
2 K. Xue, X. Lan, J. Wang and T. Wang, *Catal. Lett.*, 2020, **150**, 3234.
3 R. M. Mironenko, V. A. Likholobov and O. B. Belskaya, *Russ. Chem. Rev.*, 2022, **91**, RCR5017.
4 G. Wang, H. Xin, Q. Wang, P. Wu and X. Li, *J. Catal.*, 2020, **382**, 1.
5 S. Qiao, X. Liu, Y. Zhou, H. Wang, L. Zhang and W. Wang, *ChemistrySelect*, 2020, **5**, 5162.
6 P. V. Markov, N. S. Smirnova, G. N. Baeva, A. V. Bukhtiyarov, I. S. Mashkovsky and A. Yu. Stakheev, *Mendeleev Commun.*, 2020, **30**, 468.
7 S. Wei, Y. Zhao, G. Fan, L. Yang and F. Li, *Chem. Eng. J.*, 2017, **322**, 234.
8 S. Damyanova, B. Pawelec, K. Arishtirova, M. V. Martínez Huerta and J. L. G. Fierro, *Appl. Catal., A*, 2008, **337**, 86.
9 S. Bhogeswararao and D. Srinivas, *J. Catal.*, 2012, **285**, 31.
10 K. Vikanova, E. Redina, G. Kapustin, M. Chernova, O. Tkachenko, V. Nissenbaum and L. Kustov, *ACS Sustainable Chem. Eng.*, 2021, **9**, 1161.
11 E. A. Redina, K. V. Vikanova, G. I. Kapustin, I. V. Mishin, O. P. Tkachenko and L. M. Kustov, *Eur. J. Org. Chem.*, 2019, 4159.
12 J. Ouyang, Z. Zhao, H. Yang, J. He and S. L. Suib, *J. Hazard. Mater.*, 2019, **366**, 54.
13 A. Wolfbeisser, O. Sophiphun, J. Bernardi, J. Wittayakun, K. Föttinger and G. Rupprechter, *Catal. Today*, 2016, **277**, 234.
14 N. D. Evdokimenko, A. L. Kustov, K. O. Kim, I. V. Mishin, V. D. Nissenbaum, G. I. Kapustin, T. R. Aymaletdinov and L. M. Kustov, *Funct. Mater. Lett.*, 2020, **13**, 2040004.

15 Y.-Z. Xiang, Y.-A. Lv, T.-Y. Xu, X.-N. Li and J.-G. Wang, *J. Mol. Catal. A: Chem.*, 2011, **351**, 70.
16 F. Zhang, C.-H. Chen, J. C. Hanson, R. D. Robinson, I. P. Herman and S.-W. Chan, *J. Am. Ceram. Soc.*, 2006, **89**, 1028.
17 E. N. Kablov, A. S. Chainikova, N. E. Shchegoleva, D. V. Grashchenkov, V. S. Kovaleva and I. O. Belyachenkov, *Inorg. Mater.*, 2020, **56**, 1065.
18 M. Boniecki, T. Sadowski, P. Gołębiewski, H. Węglarz, A. Piątkowska, M. Romaniec, K. Krzyżak and K. Łosiewicz, *Ceram. Int.*, 2020, **46**, 1033.
19 N. L. Savchenko, T. Yu. Sablina, I. N. Sevost'yanova, A. G. Burlachenko, S. P. Buyakova and S. N. Kul'kov, *Tech. Phys. Lett.*, 2018, **44**, 663.
20 R. Prins, *Chem. Rev.*, 2012, **112**, 2714.
21 S. Damyanova, B. Pawelec, K. Arishtirova, M. V. Martínez Huerta and J. L. G. Fierro, *Appl. Catal., B*, 2009, **89,** 149.
22 Q. Wu, J. Ba, X. Yan, J. Bao, Z. Huang, S. Dou, D. Dai, T. Tang, W. Luo and D. Meng, *Catal. Commun.*, 2017, **98**, 34.
23 C. E. Hori, H. Permana, K. Y. Simon Ng, A. Brenner, K. More, K. M. Rahmoeller and D. Belton, *Appl. Catal., B*, 1998, **16**, 105.
24 P. Hartmann, T. Brezesinski, J. Sann, A. Lotnyk, J.-P. Eufinger, L. Kienle and J. Janek, *ACS Nano*, 2013, **7**, 2999.
25 N. Zhang, Q. Shao, P. Wang, X. Zhu and X. Huang, *Small*, 2018, **14**, 1704318.
26 B. F. Machado, S. Morales-Torres, A. F. Pérez-Cadenas, F. J. Maldonado-Hódar, F. Carrasco-Marín, A. M. T. Silva, J. L. Figueiredo and J. L. Faria, *Appl. Catal., A*, 2012, **425**–**426**, 161.
27 S. Padmanaban, Y. Lee and S. Yoon, *J. Ind. Eng. Chem.*, 2021, **94**, 361.

Received: 30th December 2021; Com. 21/6784